Biosensors and Bioelectronics 65 (2015) 257–264

Contents lists available at ScienceDirect

Biosensors and Bioelectronics

journal homepage: www.elsevier.com/locate/bios

Chemostat-like microfluidic platform for highly sensitive detection of heavy metal ions using microbial biosensors

Minseok Kim [a,1], Ji Won Lim [b,1], Hyun Ju Kim [c,d], Sung Kuk Lee [b], Sang Jun Lee [c,d,*], Taesung Kim [a,b,**]

[a] Department of Mechanical Engineering, Ulsan National Institute of Science and Technology (UNIST), 50 UNIST-gil, Eonyang-eup, Ulsan 689-798, Republic of Korea
[b] Department of Biomedical Engineering, Ulsan National Institute of Science and Technology (UNIST), 50 UNIST-gil, Eonyang-eup, Ulsan 689-798, Republic of Korea
[c] Biosystems and Bioengineering Program, University of Science and Technology, 125 Gwahak-ro, Yuseong-gu, Daejeon 305-806, Republic of Korea
[d] Infection and Immunity Research Center, Korea Research Institute of Bioscience and Biotechnology (KRIBB), 125 Gwahak-ro, Yuseong-gu, Daejeon 305-806, Republic of Korea

ARTICLE INFO

Article history:
Received 7 August 2014
Received in revised form
8 October 2014
Accepted 13 October 2014
Available online 18 October 2014

Keywords:
Microfluidic platform
Heavy metal ions
Microbial biosensor
Chemostat
Gene expression

ABSTRACT

Reporter-gene-based microbial biosensors have high potential for detecting small molecules, including heavy metal ions (HMIs), in a sensitive and selective manner by involving low costs. However, the sensitivity and dynamic range of the sensing mechanism are largely limited by the conventional culture environment that relies on the batch-type addition of the small molecules in nutrients and the subsequent genetic induction of sensing microbes. Here, we describe a high-throughput, chemostat-like microfluidic platform that can continuously supply both nutrients and inducers (HMIs) using microfabricated ratchet structures and a mixing microchannel network. We found that the microfluidic platform not only allowed microbial biosensors to be highly concentrated in a detection microchamber array but also enabled them to continuously grow and control synthetic genetic circuits in response to heavy metals. We also demonstrated that the combination of the platform and microbial biosensors enhanced the sensitivity for detecting divalent lead and cadmium ions by approximately three orders of magnitude relative to conventional batch-type methods. Because the platform is portable and only requires small sample volumes and fluorescent detection, the chemostat-like microfluidic platform in conjunction with microbial biosensors could be widely utilized to facilitate the specific and sensitive detection of molecular analytes on a chip.

1. Introduction

Sensitive and selective detection of toxic compounds and heavy metals is of significant importance for human health and the preservation and conservation of environment. In particular, heavy metals such as cadmium, mercury, and lead are found in many industrial wastes, including vehicle emissions, lead-acid batteries, and chemical fertilizers, and they are generally denser than iron. Heavy metals are toxic to cells mostly via oxidative stress (Cuypers et al., 2010; Ercal et al., 2001) and accumulate in animal bodies over time, causing lung cancer (Coen et al., 2001), brain dysfunction (Karri et al., 2008), softening of bones (Duruibe et al., 2007), and kidney disease (Roels et al., 1989). Generally, detection of heavy metal ions (HMIs) using conventional methods needs skilled operation and methods requiring expensive instruments such as atomic absorption spectroscopy (Jackson and Chen, 1996) and coupled plasma-atomic emission/mass spectroscopy (Burlingame et al., 1996), in addition to complex configuration of electrochemical instruments (Anderson et al., 1996). To overcome the limitations of the conventional methods, microbial biosensors, which utilize pre-engineered genetic circuits of live microbes, have been utilized with the rapid growth of synthetic biology (D'Souza, 2001; Lei et al., 2006; Su et al., 2011).

Microbial biosensors offer considerable advantages: they allow inexpensive and facile detection without complex equipment and provide flexibility for various analyses, and pre- and/or post-processes

* Corresponding author at: Infection and Immunity Research Center, Korea Research Institute of Bioscience and Biotechnology (KRIBB), 125 Gwahak-ro, Yuseong-gu, Daejeon 305-806, Republic of Korea.
** Corresponding author at: Department of Mechanical Engineering, Ulsan National Institute of Science and Technology (UNIST), 50 UNIST-gil, Eonyang-eup, Ulsan 689-798, Republic of Korea.
E-mail addresses: leesj@kribb.re.kr (S.J. Lee), tskim@unist.ac.kr (T. Kim).
[1] These authors contributed equally to this work.

http://dx.doi.org/10.1016/j.bios.2014.10.028
0956-5663/

such as purification and separation are not required. For example, microbial fluorescence-based (Amaro et al., 2014; Castillo et al., 2004; Tao et al., 2013) and luminescence-based biosensors (Leth et al., 2002; Shetty et al., 2003) utilize the expression of reporter genes that can be specifically switched on by biochemical interaction events between cellular receptors and inducer molecules. The optical or fluorescent signals produced by the microbes can be directly quantified during the incubation of the microbes with test solutions, thereby enabling easy, sensitive and inexpensive detection of target analytes with unknown concentrations. In addition to the fluorescent or optical signals, for the in situ detection of HMIs, several transducers were attempted to measure amperometic (Wang et al., 2013) and acoustic (Gammoudia et al., 2014) signals from the microbes that were exposed to HMIs. These biosensors showed rapid response time and high sensitivity in detection but appear to be somewhat complex and expensive for measuring electrochemical and physical signals.

Recently, bioreactor systems have been miniaturized to not only shorten diffusion distances and enhance reaction kinetics but also reduce the labor involved and sample consumption. For example, Gu et al. introduced a milliliter-scale bioreactor (58 mL working volume) that can be operated in a continuous and repeatable manner for testing toxic compounds in an aqueous solution. They found that higher growth rates and/or dilution rates enhanced the performance of microbial biosensors (Gu et al., 1996). Additionally, Charrier et al. reported a bioreactor system with multiple wells that had a diameter of several millimeters and were connected in series. They immobilized microbial biosensors in the multiple wells and then applied a sample solution containing several heavy metals to utilize the biosensors to express bioluminescence in response to the target analytes (Charrier et al., 2011). For further miniaturization, several research groups developed microfluidic devices and combined them with microbial biosensors for detecting toxic compounds and HMIs. For instance, Rothert et al. (2005) used a microbial whole-cell biosensor in a centrifugal microfluidic device to detect six different conditions of HMIs such as arsenite and antimonite by generating selective fluorescence signals from the biosensors. In addition, Garcia-Alonso et al. (2011, 2009) prepared a microfluidic device that had several microchannels in parallel and could screen multiple toxic compounds or a single compound at different concentrations on a chip by using chemical gradients and recombinant yeast cells. These approaches combining a microbial biosensor and a miniaturized device/system provided many advantages, including small sample volume consumption and short analysis time (Garcia-Alonso et al., 2011, 2009; Rothert et al., 2005), high throughput (Charrier et al., 2011; Garcia-Alonso et al., 2011, 2009; Rothert et al., 2005), and enhanced sensitivity and selectivity, compared to conventional methods (Gu et al., 1996; Rothert et al., 2005). However, most of these approaches appear to rely on conventional batch-mode culture environments.

Basically, the batch-type mixing of microbes and target analytes in a confined solution not only limits the maximum cell growth because of depletion of nutrients but also gradually reduces the number of target analytes available for additional induction over time. In contrast, it is advantageous to provide a continuous nutrient environment for microbes to enable high cell growth rates in a microchamber on a chip (Groisman et al., 2005). For this reason, a continuous culture and induction environment is essential to enhance detection sensitivity because continuous feeding of nutrients and target analytes (target HMIs) helps enhance the gene expression in the microbial biosensor. For these reasons, in this study, we developed a microfluidic device that not only concentrates motile microbes in a compartmentalized microchamber array but also grows the concentrated microbes in a continuous-feed mode. For the self-concentration of microbes in the microchamber array, we utilized a microfabricated, arrowhead-shaped ratchet structure and the intrinsic tendency of microbes to swim on the right side, which has been well demonstrated in our previous studies (Kim et al., 2010; Park et al., 2012). For the continuous-feed mode, this novel device enabled the feeding of nutrients and various concentrations of HMIs (e.g. Pb^{2+} and Cd^{2+}) in the compartmentalized microchambers in a continuous manner, thereby introducing a simple and convenient chemostat-like culture environment. Using the combination of the chemostat-like culture environment and synthetically engineered microbial biosensors, we characterized the sensitivity and selectivity of the microbial biosensors for detecting HMIs and then compared the result with that obtained using conventional batch-type methods.

2. Experimental

2.1. Reagents and materials

For visualization and quantification of the microfluidic channels, green, red, and yellow dyes and 50 mM fluorescein isothiocyanate (FITC) were mixed with deionized water, respectively. As the target HMI, Pb^{2+} and Cd^{2+} were prepared in a cell culture solution (tryptone broth (TB), 1% tryptone, and 0.5% NaCl) with ampicillin (75 μg/mL). A Luria broth (LB) agar plate was prepared by mixing agar (1% w/v) for colony formation. For detection of HMIs, analyte solutions of $PbCl_2$ (Cat. No. 203572) and $CdCl_2$ (Cat. No. 439800) were purchased from Sigma-Aldrich and diluted into autoclaved distilled water to the desired concentrations when necessary.

2.2. Preparation of bacterial cells

We used two *Escherichia coli* K-12 strains (MG1655 and DH5) as platform cells to develop microbial sensors. The MG1655 strain harboring pTKU4-2 plasmid that constitutively expresses green fluorescent protein (GFP) was used for testing cell growth in the chemostat-like microfluidic device. DH5α cells harboring plasmids pHK194 and pHK200 were used for detecting Pb^{2+} and Cd^{2+} and named as the HK621 and HK622 strains, respectively. For continuous induction tests in the microfluidic device, a single colony of the *E. coli* on an LB agar plate was grown in 5 mL in LB broth in a test tube that was rigorously agitated in a rotary shaking incubator (37 °C and 200 rpm) overnight. The cultured cells were then introduced into the microfluidic device through the inlet reservoirs so that they were flowed along the microchannels and then accumulated in the microchamers. For batch-type detection in test tubes, the cells were grown to mid-log phase in 5 mL of LB broth until the optical density at a wavelength of 600 nm reached $OD_{600}=0.5$ and various concentrations of the HMI were added for induction of fluorescent reporter gene expression, followed by incubation at 37 °C and 200 rpm overnight. For a fair, reasonable comparison of the batch-type biosensing method with the chemostat-like biosensing method, the cell density of the batch-type method was intentionally enhanced by centrifugation (Combi 514R, Han-Il Instrument, Incheon, Republic of Korea) at 3000 rpm for 10 min at 25 °C.

2.3. Fabrication and operation of the microfluidic device

The microfluidic device was fabricated and its channel feature was 200 μm wide and 10 μm deep. The microfluidic device consisted of a mixing channel network and a microchamber array for compartmentalized cell culture on a chip as used in our previous study (Park et al., 2012). The microchamber array was integrated with ratchet structures to physically isolate the microbes from the

main channel but chemically allow the transport of nutrients and small molecules to and from the main channel (Kim et al., 2011, 2010; Park et al., 2012). The test and control chambers were designed differently. A small pointed shape was intentionally added to the control chambers to make it easier to distinguish them from the test chambers during experiments and image processing. However, no difference was found during the cell culture and induction experiments. The microfluidic device was fabricated using standard soft lithography as used in our previous work. Briefly, an SU-8 (Microchem 2025, Newton, MA, USA) master (approximately 10 μm thick) was fabricated using standard photolithographic procedures. The surface was silanized using trichloro(3,3,3-trifluoropropyl)silane (Sigma Aldrich, Korea) in a vacuum jar for 1 h. Polydimethylsiloxane (PDMS) was then cast, cured, and peeled off to prepare the microfluidic devices. PDMS devices and glass substrates were treated with oxygen plasma under 50 sccm of O_2 and 50 W for 30 s (Cute-MP, Femto Science, Korea) prior to all the experiments. This plasma treatment made the PDMS devices irreversibly bonded to the glass substrate, resulting in tight seal of the microfluidic channels. The treatment also made all the channel surfaces hydrophilic so that aqueous solutions were flowed along the main microchannel easily and then toward the test and control chambers with a dead end. Air trapped in the dead end was easily eliminated by squeezing pressure driven by capillary forces and the high gas permeability of PDMS (5.2×10^{-6}–3.4×10^{-5} cm^2/s) (Merkel et al., 2000). As a result, no air bubbles were formed in the device.

Once bacterial cell suspension was loaded into the test and control chambers, the cells were not allowed to escape from them due to the guiding/redirecting function of the ratchet structure and the motility of the cells. After the cells were trapped in the chambers a solution containing nutrients and target HMIs was continuously flushed by using the hydrostatic heads of the inlet reservoirs. The hydrostatic heads of the outlets were maintained to be lower than the inlets so that spent fluids automatically come out of the device and then discarded safely.

2.4. Experimental setup and data analysis

An inverted fluorescence microscope (Ti-U, Nikon, Tokyo, Japan) equipped with a CCD camera (ORCA R2, Hamamatsu Photonics, Hamamatsu, Japan) and a 10× lens was used to measure the

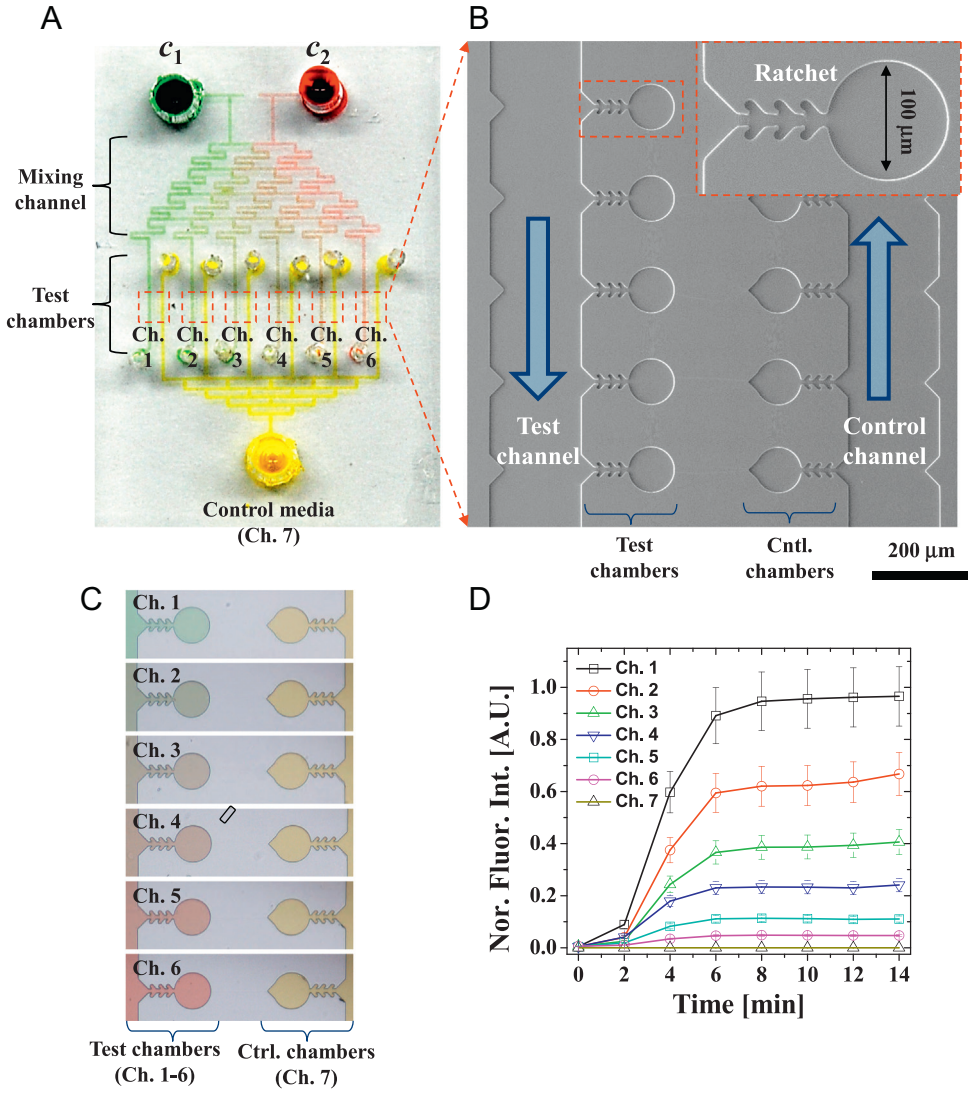

Fig. 1. A microfluidic device for microbial biosensors for detecting HMIs (Pb^{2+} and Cd^{2+}). (A) Microscopic image shows the microfluidic channels consisting of a concentration gradient generator and a microbe culture chamber array. (B) SEM image shows one set of test channels and control channels. Chambers are connected to the main channel with ratchet structures that enable chemicals and molecules to be transported but prevent motile cells in the chamber from escaping to the main channel. (C) Microscopic images to visualize concentration gradients in the test chambers and the control chambers. (D) Quantification of concentration gradients by using fluorescence intensity (50 μM FITC solution).

fluorescence from the FITC and *E. coli*. For data analysis and image processing, Image J (NIH, Bethesda, MD, USA) and OriginPro 8 (OriginLab, Northampton, MA, USA) were used when necessary.

3. Results and discussion

3.1. Generation of concentration gradients and culture chambers with ratchet structures

Fig. 1A shows the microfluidic device consisting of a mixing channel network (Park et al., 2012) and a test microchamber array. The device has 6 sets of control and test channels and each set has five cell-culture chambers in a column to minimize uncertainty in measuring fluorescent and optical signals from microbial biosensors. Fig. 1B shows a scanning electron microscope (SEM) image from Ch. 6. Each microchamber is connected to the main channel through a ratchet structure that not only guides and accumulates motile microbes from the main channel but also prevents the trapped microbes from escaping to the main channel. In addition, the ratchet structure offers a chemostat-like culture environment for the microbes to grow in a continuous-feed mode that continuously supplies fresh nutrients and inducer molecules (HMI) from the main channel to the chambers and, at the same time, washes away secreted metabolites from the chamber to the main channel. These aspects were well characterized in our previous work (Kim et al., 2010). To test the mixing channels, a solution with green food dye was loaded to the top-left reservoir (c_1) whereas a solution with red food dye was applied to the top-right reservoir (c_2). The solutions flowed along the mixing channels and mixed together, resulting in the generation of concentration gradients from Ch. 1 to Ch. 6. The control channels (Ch. 7) were positioned in parallel with each test channel for direct comparison. Fig. 1C shows that each set of test and control chambers exhibited different colors. Therefore, we confirmed that the mixing channels generate concentration gradients, suggesting utility for high-throughput assays. The concentration gradients of HMI were indirectly characterized by application of a buffer solution with fluorescein (50 μM FITC) and then quantified as shown in Fig. 1D. As designed and expected, each test channel showed different fluorescence intensities, corresponding to the following concentrations: 100% (50 μM), 63 (31.5 μM), 39 (19.5 μM), 23 (11.5 μM), 10 (5 μM), 5 (2.5 μM), and 0% (buffer only) from Ch. 1 through Ch. 7. Because the diffusivities of Pb^{2+} (0.94×10^{-9} m^2/s), (Valente et al., 2004) and Cd^{2+} (0.7×10^{-9} m^2/s) (Arefev et al., 1987) are close to the diffusivity of FITC (0.49×10^{-9} m^2/s) (Rani et al., 2005), it was presumed that the concentration of HMIs in the microfluidic device is also close to the quantified concentration of FITC.

3.2. Bacterial cell growth in a chemostat-like culture environment

We tested *E. coli* cell growth by using fresh and spent TB medium as shown in Fig. 2A to determine whether cellular growth was affected by continuous feeding of nutrients. Because the microfluidic device can generate various concentration gradients as designed, a single experiment provided six different culture conditions plus a control on a chip. We monitored the growth of *E. coli* cells that constitutively express green fluorescent protein (GFP) using a fluorescent microscope, as shown in Fig. 2B, and then found that cellular growth properly increased in the chambers as nutrients were continuously supplied. Fig. 2C shows the quantified fluorescence intensities corresponding to the cell growth results presented in Fig. 2B. At $t=0$ h, the number of fluorescent *E. coli* cells in each microchamber appeared to be unbiased. However, the fluorescence intensities, although they only indirectly represent the growth rate of the cells in each chamber, significantly changed over time in every chamber. For Ch. 1, in which 100% fresh medium was added (continuous feed mode), the fluorescent intensities showed an exponential increase between 3 h and 7 h, which is likely to be proportional to the increase in the number of fluorescent cells. In contrast, for Ch. 7, in which 100% spent TB medium was added (similar to the batch-type mode), the fluorescent intensities did not increase and remained almost constant over time. For other various intermediate conditions, the growth rates appeared to be accurately proportional to the nutrient gradients.

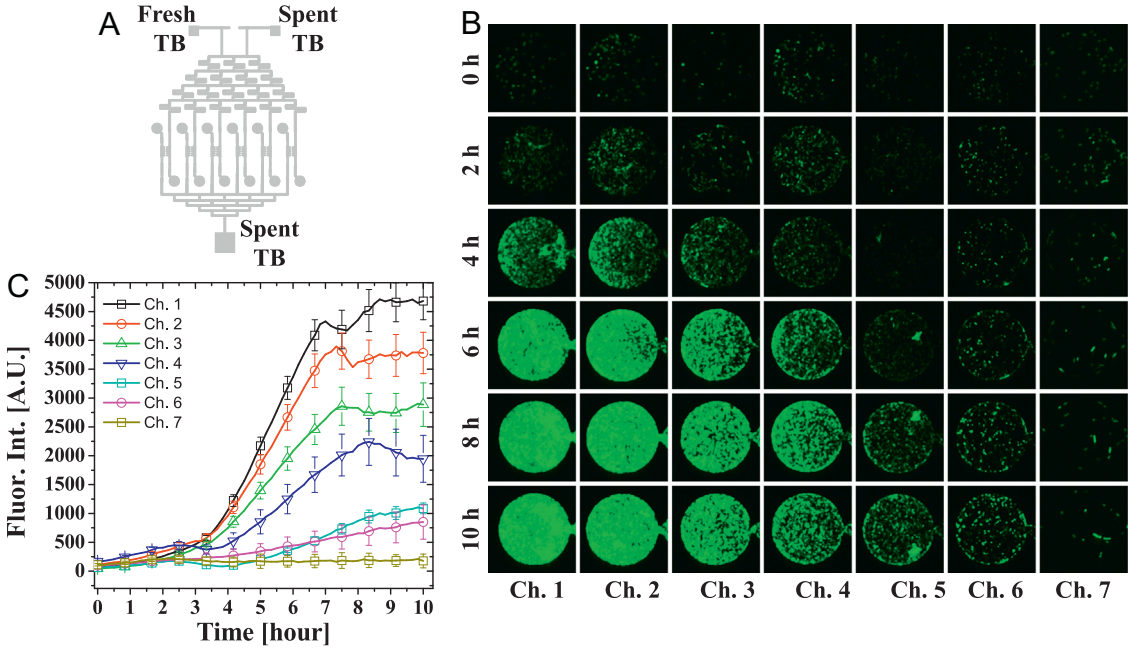

Fig. 2. Bacterial cell growth (*E. coli*) in continuous-feed and batch modes. (A) A schematic image showing experimental conditions in which concentration gradients of fresh TB media and spent TB media are produced at the same time from left to right and vice versa. (B) Fluorescent time-lapse images show cell growth in various nutrient-feeding conditions. Ch. 1 represents a continuous-feed mode (100% fresh TB), whereas Ch. 7 (control) represents a batch-type mode (100% spent TB). (C) Quantification of GFP signals of the cells in the chambers reveal various growth rates determined by the mixing ratios (concentrations) of the fresh and used TB.

Even though fully grown fluorescent cells, after overnight incubation in a test tube, were injected into the device, we observed further cell growth in the microchambers as nutrients were supplied. Additionally, the fluorescent cells were not able to escape from the microchambers with the ratchet structure, but nutrients and metabolites could freely diffuse into and out of the microchambers. We confirmed that the chemostat-like cell culture environment dramatically increased the cell density on the chip, which in turn was helpful to improve the performance of the microbial biosensors for HMI detection compared to conventional cell culture environments such as test tubes and microplate instruments that only allow a batch-type culture environment. This remarkable rise of cell growth may play a key role in increasing the biosensing sensitivity because intense fluorescence signals were measured in response to target HMIs that were continuously delivered in the microchambers.

3.3. Characterization of gene expression level to detect HMIs

We employed two types of microbial whole-cell biosensors that harbored artificially engineered plasmids for detection of Pb^{2+} or Cd^{2+} in solution. The detection mechanism was based on the negative control of the GFP reporter gene mediated by CadC-type transcriptional repressors, which bind to Pb^{2+} or Cd^{2+} divalent ions and derepress the GFP reporter promoters. Two *cadC* transcriptional modules were cloned from the genome of *Bacillus oceanisediminis* 2691. We characterized the microbial biosensors HK621 for Pb^{2+} ions and HK622 for Cd^{2+} ions using the microfluidic device. HMIs dissolved in TB medium (20 μM) were introduced to the left-top reservoirs and only TB media was introduced to the right-top and right-bottom control reservoirs. As shown in Fig. 3A and C, each microfluidic device was used for seven different detection experiments on a chip with various concentrations of Pb^{2+} ions. After 5 h of cell culture, the fluorescent intensities showed a linear dependency on the concentration of the Pb^{2+} ion; a higher concentration was associated with stronger fluorescence intensity. After 10 h, the differences among the normalized fluorescence intensities from Ch. 1 to Ch. 6 appeared to decrease. This effect was attributed to the continuous supplementation with Pb^{2+} ions, which activated microbial transcription to over-express the biosensor construct and trigger the accumulation of GFP within the cells. For Cd^{2+} ion detection, we found that the fluorescence intensities showed a nonlinear dependency on the concentration of Cd^{2+} ions as shown in Fig. 3B and D. The plasmid activity and cell growth appeared to be affected by high concentrations of Cd^{2+} ions in solution. However, the continuous-feed culture showed increased fluorescence intensities, especially with low concentrations of metal ions. It could

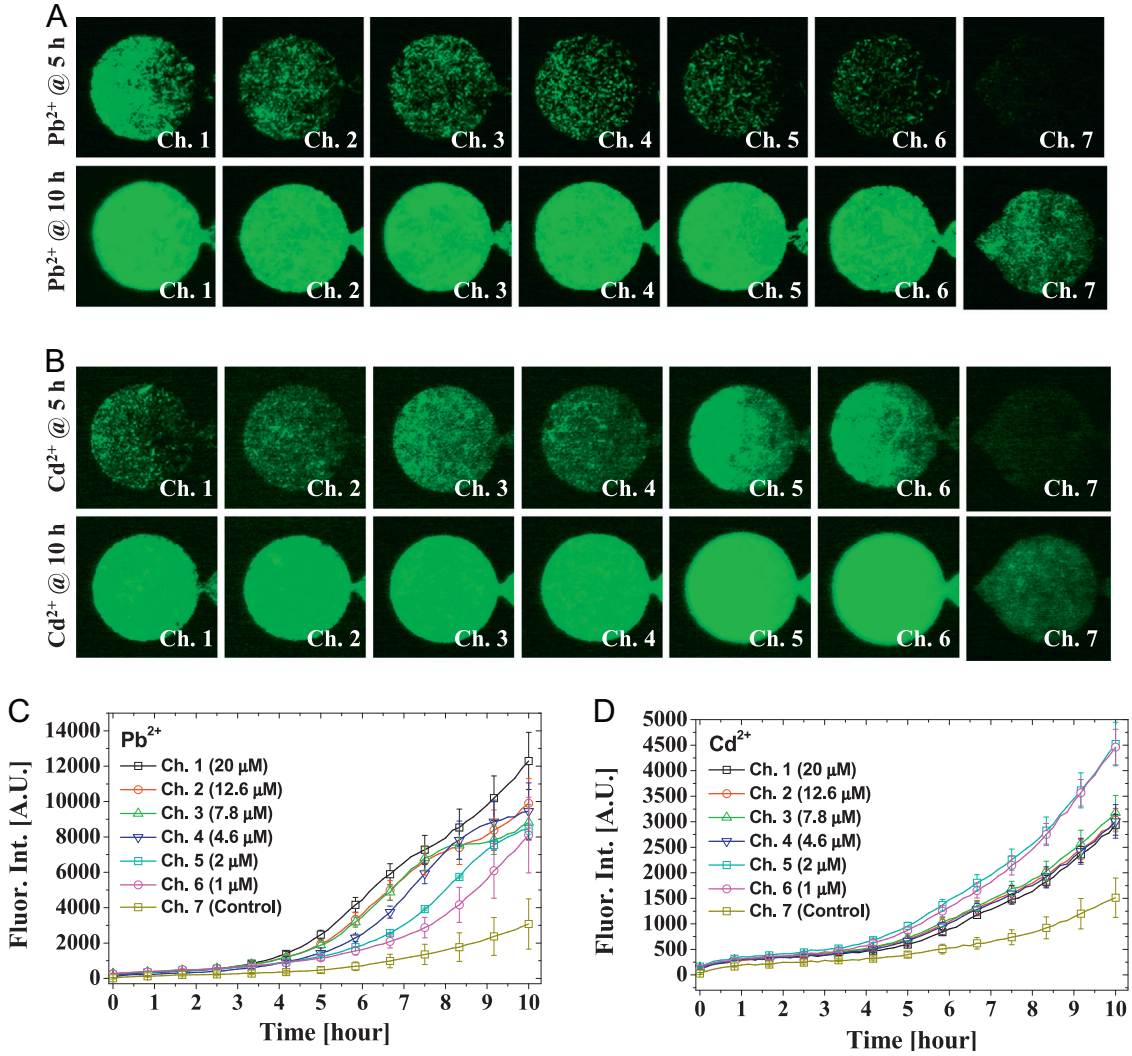

Fig. 3. Detection of HMIs by the microfluidic device and the microbial biosensors. (A) and (C) Detection of Pb^{2+} ions using *E. coli* HK621 cells at various concentrations ranging from 20 μM to 0 μM (control). (B) and (D) Detection of Cd^{2+} ions using *E. coli* HK622 cells at various concentrations ranging from 20 μM to 0 μM (control). The fluorescent intensities depended on the concentrations of HMIs over time.

therefore be speculated that Cd^{2+} ions gradually accumulate in cells up to a concentration sufficient to turn on the reporter gene without interfering with cellular growth. On the other hand, when the concentration of Cd^{2+} ions was relatively high, corresponding fluorescence intensities were not linearly proportional to them. Possible reasons can be attributed to different heavy metal toxicity. It was previously reported that 50% inhibitory concentrations (i.e. IC_{50}) of $CdCl_2$ and $PbCl_2$ are 2.3 and 569.0 ppm, respectively, when added to *E. coli* culture. This result indicates that the toxicity of Cd^{2+} ions to bacterial cells is severer than that of Pb^{2+} (Chao et al., 1995). Due to the chemostat-like microfluidic device, it appears that HMIs gradually and substantially accumulated in cells over time. Therefore, not only might intracellular Cd^{2+} be much higher than the concentration of the feeding solution but also the more accumulation of Cd^{2+} might cause growth retardation or cellular toxicity, which resulted in the lower and irregular expression of GFP in cells at high concentrations of Cd^{2+} ions. Further study and engineering for high-sensitive microbial cells would be required to address this toxicity issue clearly but we demonstrated that the combination of the microfluidic device and the microbial biosensors improved the sensitivity and the dynamic range for HMI detection.

3.4. Comparison of continuous induction and batch-type induction for HMI detection

The detection performance for HMIs using the microfluidic device was compared to that of the conventional detection method using batch culture under the same microscopic imaging conditions. First, we obtained the fluorescence intensities from the microbial biosensors for different concentrations of Pb^{2+} ions (20 μM, 200 nM, and 2 nM; none as a negative control) after 10 h of incubation in the chemostat-like environment as shown in Fig. 4A and B. Because the device enabled continuous supplementation of nutrients and maintained Pb^{2+} ions in their initial state in the detection chambers, the increase of fluorescence signals by approximately 4–5 fold was obtained when compared with the control experiment (without HMI) even at low concentrations such as 200 nM and 2 nM. However, the batch-type induction did not produce sufficient fluorescence signals to enable differentiation from the control signal because of the lower cell density and limited supplementation of Pb^{2+} ions. An alternative method of increasing the signal difference in the batch-type induction method was demonstrated by increasing the cell density by a factor of 15 using an external centrifuge as described in Section 2 (Section 2.2). However, the fluorescence signals in the 15 × batch-type induction were still much lower than those in the continuous induction. Moreover, this method required an additional cell-concentrating step with increasing sample consumption and labor. Similar to the findings during Pb^{2+} detection, Cd^{2+} ions showed a higher signal-to-noise ratio in the continuous induction method than in the batch-induction method, as shown in Fig. 4C and D. Therefore, the microbial biosensors with the continuous chemostat-like environment improved the sensitivity and dynamic range of the microbial biosensors by approximately three orders of magnitude compared to the conventional batch-induction method for detecting HMIs (Corbisier et al., 1999). The enhanced performance can be attributed to the continuous expression of the

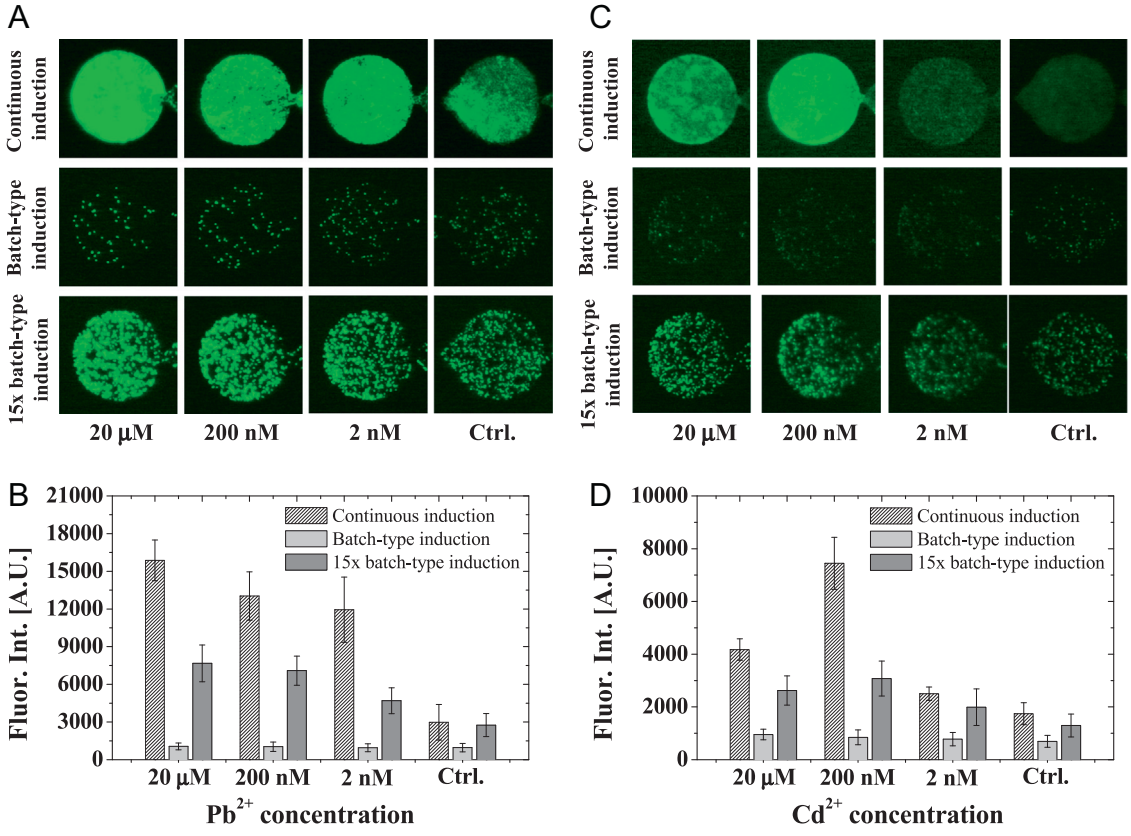

Fig. 4. Comparison between continuous and batch-type induction of microbial biosensors. (A) and (B) Continuous and batch-type induction of *E. coli* HK621 cells in various concentrations of Pb^{2+} ions such as 20 μM, 200 nM, 2 nM, and 0 nM as a control. In continuous induction, the microbial cells were grown and treated with inducer molecules (Pb^{2+} ions) in the chemostat-like microfluidic device for 10 h. The batch-type induction and 15 × accumulated batch-type induction were performed in conventional batch-type culture tubes for 10 h, and then the induced microbial cells were loaded into the microfluidic device for immediate fluorescent measurements. The 15 × concentration enhancement was achieved by using a centrifuge immediately before loading into the microfluidic device. (C) and (D) Induction of *E. coli* HK622 cells in various concentrations of Cd^{2+} ions. All fluorescence images were obtained under the same microscopic configurations.

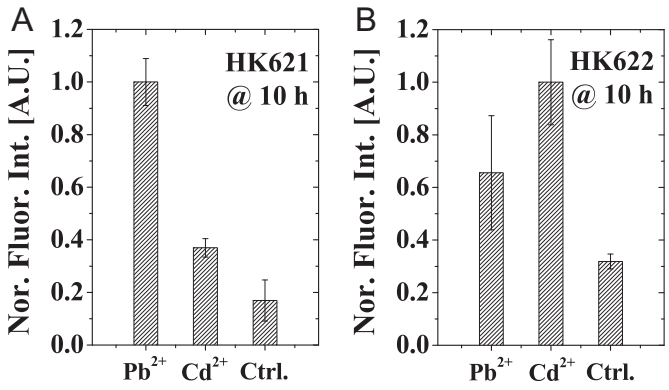

Fig. 5. High-throughput characterization of the selectivity and cross-talk of the two microbial biosensor cells, HK621 and HK622, respectively, using the microfluidic device. (A) Induction of the HK621 biosensor in a solution containing both 20 μM Pb^{2+} and 20 μM Cd^{2+} ions after 10 h. (B) Induction of the HK622 biosensor in the same solution after 10 h. The fluorescence intensities measured under the same microscopic conditions were normalized by the maximum fluorescence intensity value.

engineered genes and the larger number of cells in the detection chamber. Even with a low concentration of HMI (e.g. 2 nM), the genes appeared to be repeatedly activated over time by continuous supplementation and/or intracellular accumulation of the target HMI, resulting in over-expression of GFP in the cells (Andersen et al., 1998).

3.5. *Characterization of the selectivity of the microbial biosensors*

The microfluidic device enables diverse characterizations of microbial biosensors in various HMI conditions. For example, to confirm the selectivity of the microbial biosensor, we tested each type of microbial cells with a non-target HMI; the microbial sensor cells that were designed for Pb^{2+} detection were exposed to a solution containing both 20 μM Pb^{2+} and 20 μM Cd^{2+} and vice versa. As described in Fig. 5, the microbial biosensors showed the maximum fluorescent intensity in the target HMI conditions, indicating heavy metal selectivity. Although the results with the non-target HMI showed a low amount of fluorescence intensity caused by leaky expression or non-specific removal of the repressor on the *cad*C gene in the engineered microbes, the microfluidic device provides a quantitative platform with remarkable potential to characterize the whole-cell-based biosensing system in various HMI conditions with considerably decreased response time and reduced sample consumption.

3.6. *Potential application of the microfluidic device and microbial biosensors*

The combination of the microfluidic device and the bacterial biosensors could be very useful for detecting HMIs in a small volume of samples or tiny environmental compounds. As the target sample can be mixed with nutrient media, this mixing process may decrease the final working concentration but increase the working volume. Because the microfluidic device makes it possible to detect very low concentrations of HMIs, the application of this approach may not be limited to the small volume of samples. In addition, we note that the microfluidic device and bacterial biosensors have remarkable potential to be a portable biosensor because not only can the microfluidic device be operated by hydrostatic heads without any external pumping system but also integrated with a portable CCD camera system (Roda et al., 2013) for fluorescent detection. It is obvious that the microbial biosensors can be synthetically engineered to produce stronger fluorescence signals in response to metal ions for enhanced sensitivity and selectivity (Wu et al., 2009).

4. Conclusions

We developed a microfluidic platform that consisted of a micromixer to generate concentration gradients of HMIs and a microchamber array with a ratchet structure to concentrate and compartmentalize motile microbial whole-cell biosensors. The microfluidic platform provided a chemostat-like culture environment with the microbial biosensors such that an extremely high cell population (density) in each microchamber was achieved because the cells grew well in a continuous feed mode. In addition, the culture environment enabled higher reporter gene expression in the cells, enhancing the sensitivity and dynamic range by three to four orders of magnitude for detection of Pb^{2+} and Cd^{2+} when compared to conventional batch-type feeding and induction methods. This increase was achieved because the microfluidic platform not only provided fresh solutions containing nutrients and HMIs to the compartmentalized microbial biosensors but also simultaneously removed secreted metabolites. Notably, the total amount of the solutions used was much lower than that with other conventional methods (e.g. only 200 μL was required for 6 experiments on a chip basis, compared to one sample in a 5 mL tube in conventional experiment). Moreover, the combination of the chemostat-like microfluidic platform and synthetic microbial biosensors offered remarkable advantages compared to conventional biosensors for detecting HMIs (1) cost-effective and time-reduced detection without complex equipment, (2) flexibility for multiplex detection in a high-throughput manner, and (3) direct and convenient measurement without pre- or post-treatment of sample solutions.

Acknowledgments

This work was supported by Grants from the Next-Generation BioGreen 21 program (SSAC, PJ00954905 and PJ009524), Rural Development Administration, Republic of Korea.

References

Amaro, F., Turkewitz, A.P., Martin-Gonzalez, A., Gutierrez, J.C., 2014. Functional GFP-metallothionein fusion protein from Tetrahymena thermophila: a potential whole-cell biosensor for monitoring heavy metal pollution and a cell model to study metallothionein overproduction effects. Biometals 27 (1), 195–205.
Andersen, J.B., Sternberg, C., Poulsen, L.K., Bjorn, S.P., Givskov, M., Molin, S., 1998. New unstable variants of green fluorescent protein for studies of transient gene expression in bacteria. Appl. Environ. Microb. 64 (6), 2240–2246.
Anderson, J.L., Bowden, E.F., Pickup, P.G., 1996. Dynamic electrochemistry: methodology and application. Anal. Chem. 68 (12), R379–R444.
Arefev, K.M., Guseva, M.A., Khomchenkov, B.M., 1987. Determination of the coefficient of diffusion of cadmium and magnesium vapors in gases by the Stefan method. High Temp. 25 (2), 174–179.
Burlingame, A.L., Boyd, R.K., Gaskell, S.J., 1996. Mass spectrometry. Anal. Chem. 68 (12), R599–R651.
Castillo, J., Gaspar, S., Leth, S., Niculescu, M., Mortari, A., Bontidean, I., Soukharev, V., Dorneanu, S.A., Ryabov, A.D., Csoregi, E., 2004. Biosensors for life quality – design, development and applications. Sens. Actuator B – Chem. 102 (2), 179–194.
Chao, X., Jing, Y., Heping, X., 1995. Effects of lead, cadmium, mercury chlorides and aquatic environmental samples on the growth of *Escherichia coli*. J. Environ. Sci. 7 (4), 455–460.
Charrier, T., Chapeau, C., Bendria, L., Picart, P., Daniel, P., Thouand, G., 2011. A multichannel bioluminescent bacterial biosensor for the on-line detection of metals and toxicity. Part II: technical development and proof of concept of the biosensor. Anal. Bioanal. Chem. 400 (4), 1061–1070.
Coen, N., Mothersill, C., Kadhim, M., Wright, E.G., 2001. Heavy metals of relevance to human health induce genomic instability. J. Pathol. 195 (3), 293–299.

Corbisier, P., van der Lelie, D., Borremans, B., Provoost, A., de Lorenzo, V., Brown, N. L., Lloyd, J.R., Hobman, J.L., Csoregi, E., Johansson, G., Mattiasson, B., 1999. Whole cell- and protein-based biosensors for the detection of bioavailable heavy metals in environmental samples. Anal. Chim. Acta 387 (3), 235–244.

Cuypers, A., Plusquin, M., Remans, T., Jozefczak, M., Keunen, E., Gielen, H., Opdenakker, K., Nair, A.R., Munters, E., Artois, T.J., Nawrot, T., Vangronsveld, J., Smeets, K., 2010. Cadmium stress: an oxidative challenge. Biometals 23 (5), 927–940.

D'Souza, S.F., 2001. Microbial biosensors. Biosens. Bioelectron. 16 (6), 337–353.

Duruibe, J.O., Ogwuegbu, M.O.C., Egwurugwu, J.N., 2007. Heavy metal pollution and human biotoxic effects. Int. J. Phys. Sci. 2 (5), 112–118.

Ercal, N., Gurer-Orhan, H., Aykin-Burns, N., 2001. Toxic metals and oxidative stress part I: mechanisms involved in metal-induced oxidative damage. Curr. Top. Med. Chem. 1 (6), 529–539.

Gammoudia, I., Raimbault, V., Tarbague, H., Morote, F., Grauby-Heywang, C., Othmane, A., Kalfat, R., Moynet, D., Rebiere, D., Dejous, C., Cohen-Bouhacina, T., 2014. Enhanced bio-inspired microsensor based on microfluidic/bacterial/love wave hybrid structure for continuous control of heavy metals toxicity in liquid medium. Sens. Actuator B – Chem. 198, 278–284.

Garcia-Alonso, J., Fakhrullin, R.F., Paunov, V.N., Shen, Z., Hardege, J.D., Pamme, N., Haswell, S.J., Greenway, G.M., 2011. Microscreening toxicity system based on living magnetic yeast and gradient chips. Anal. Bioanal. Chem. 400 (4), 1009–1013.

Garcia-Alonso, J., Greenway, G.M., Hardege, J.D., Haswell, S.J., 2009. A prototype microfluidic chip using fluorescent yeast for detection of toxic compounds. Biosens. Bioelectron. 24 (5), 1508–1511.

Groisman, A., Lobo, C., Cho, H.J., Campbell, J.K., Dufour, Y.S., Stevens, A.M., Levchenko, A., 2005. A microfluidic chemostat for experiments with bacterial and yeast cells. Nat. Methods 2 (9), 685–689.

Gu, M.B., Dhurjati, P.S., VanDyk, T.K., LaRossa, R.A., 1996. A miniature bioreactor for sensing toxicity using recombinant bioluminescent *Escherichia coli* cells. Biotechnol. Progr. 12 (3), 393–397.

Jackson, K.W., Chen, G.R., 1996. Atomic absorption, atomic emission, and flame emission spectrometry. Anal. Chem. 68 (12), R231–R256.

Karri, S.K., Saper, R.B., Kales, S.N., 2008. Lead encephalopathy due to traditional medicines. Current. Drug Saf. 3 (1), 54–59.

Kim, M., Kim, S.H., Lee, S.K., Kim, T., 2011. Microfluidic device for analyzing preferential chemotaxis and chemoreceptor sensitivity of bacterial cells toward carbon sources. Analyst 136 (16), 3238–3243.

Kim, S.Y., Lee, E.S., Lee, H.J., Lee, S.Y., Lee, S.K., Kim, T., 2010. Microfabricated ratchet structures for concentrating and patterning motile bacterial cells. J. Micromech. Microeng. 20, 9.

Lei, Y., Chen, W., Mulchandani, A., 2006. Microbial biosensors. Anal. Chim. Acta 568 (1-2), 200–210.

Leth, S., Maltoni, S., Simkus, R., Mattiasson, B., Corbisier, P., Klimant, I., Wolfbeis, O. S., Csoregi, E., 2002. Engineered bacteria based biosensors for monitoring bioavailable heavy metals. Electroanalysis 14 (1), 35–42.

Merkel, T.C., Bondar, V.I., Nagai, K., Freeman, B.D., Pinnau, I., 2000. Gas sorption, diffusion, and permeation in poly(dimethylsiloxane). J. Polym. Sci. Pol. Phys. 38 (3), 415–434.

Park, S., Hong, X.Q., Choi, W.S., Kim, T., 2012. Microfabricated ratchet structure integrated concentrator arrays for synthetic bacterial cell-to-cell communication assays. Lab Chip 12 (20), 3914–3922.

Rani, S.A., Pitts, B., Stewart, P.S., 2005. Rapid diffusion of fluorescent tracers into Staphylococcus epidermidis biofilms visualized by time lapse microscopy. Antimicrob. Agents Chemother. 49 (2), 728–732.

Roda, A., Cevenini, L., Borg, S., Michelini, E., Calabretta, M.M., Schuler, D., 2013. Bioengineered bioluminescent magnetotactic bacteria as a powerful tool for chip-based whole-cell biosensors. Lab Chip 13 (24), 4881–4889.

Roels, H.A., Lauwerys, R.R., Buchet, J.P., Bernard, A.M., Vos, A., Oversteyns, M., 1989. Health significance of cadmium induced renal dysfunction-a 5 year follow up. Br. J. Ind. Med. 46 (11), 755–764.

Rothert, A., Deo, S.K., Millner, L., Puckett, L.G., Madou, M.J., Daunert, S., 2005. Whole-cell-reporter-gene-based biosensing systems on a compact disk microfluidics platform. Anal. Biochem. 342 (1), 11–19.

Shetty, R.S., Deo, S.K., Shah, P., Sun, Y., Rosen, B.P., Daunert, S., 2003. Luminescence-based whole-cell-sensing systems for cadmium and lead using genetically engineered bacteria. Anal. Bioanal. Chem. 376 (1), 11–17.

Su, L.A., Jia, W.Z., Hou, C.J., Lei, Y., 2011. Microbial biosensors: a review. Biosens. Bioelectron. 26 (5), 1788–1799.

Tao, H.C., Peng, Z.W., Li, P.S., Yu, T.A., Su, J., 2013. Optimizing cadmium and mercury specificity of CadR-based *E-coli* biosensors by redesign of CadR. Biotechnol. Lett. 35 (8), 1253–1258.

Valente, A.J.M., Ribeiro, A.C.F., Lobo, V.M.M., Jimenez, A., 2004. Diffusion coefficients of lead (II) nitrate in nitric acid aqueous solutions at 298 K. J. Mol. Liq. 111 (1-3), 33–38.

Wang, X., Liu, M., Wang, X., Wu, Z., Yang, L., Xia, S., Chen, L., Zhao, J., 2013. p-Benzoquinone-mediated amperometric biosensor developed with Psychrobacter sp. for toxicity testing of heavy metals. Biosens. Bioelectron. 41, 557–562.

Wu, C.H., Le, D., Mulchandani, A., Chen, W., 2009. Optimization of a whole-cell cadmium sensor with a toggle gene circuit. Biotechnol. Prog. 25 (3), 898–903.